2018 Annual American Control Conference (ACC)
June 27–29, 2018. Wisconsin Center, Milwaukee, USA

Low-complexity modeling of mode interactions in boundary layer flows

Wei Ran, Armin Zare, M. J. Philipp Hack, and Mihailo R. Jovanović

Abstract— **Low-complexity approximations of the Navier-Stokes equations have been widely used in the analysis of wall-bounded shear flows. In this paper, we augment the linear parabolized stability equations with Floquet analysis to capture mode interactions and their effect on the evolution of fluctuating quantities in the transitional boundary layer. To this end, we leverage Floquet theory by incorporating the fluctuations that arise from primary instability mechanisms into the base flow and accounting for different harmonics in the flow state. We examine the formation of streamwise elongated streaks in the presence of weakly nonlinear effects. In this process, we capture the growth of various harmonics observed in the direct numerical simulation of laminar streaks. Our proposed model provides a convenient linear progression of fluctuation dynamics in the streamwise direction and is thus well-suited for stability analysis and real-time control of spatially-evolving flows.**

Index Terms— **Boundary layers, control-oriented modeling, distributed systems, Floquet theory, parabolized stability equations, spatially-periodic systems, streaks, transitional flows.**

I. Introduction

We are interested in the control-oriented modeling of spatially evolving flows. Due to their high complexity and large number of degrees of freedom, nonlinear dynamical models that are based on the Navier-Stokes (NS) equations are not suitable for analysis, optimization, and control. On the other hand, experimentally and numerically generated data sets are becoming increasingly available for a wide range of flow configurations. This has enabled data-driven techniques for the reduced-order modeling of fluid flow systems. Despite being computationally tractable, such models often lack robustness. Specifically, control actuation and sensing may significantly alter the identified modes which introduces nontrivial challenges for model-based control design [1]. In contrast, models that are based on the linearized NS equations are less prone to such uncertainty and are, at the same time, well-suited for analysis and synthesis using tools of modern robust control [2].

The stochastically forced linearized NS equations have been used to capture structural and statistical features of transitional [3]–[5] and turbulent [6]–[8] channel flows. In these models, stochastic forcing is utilized to model the effect of nonlinear terms in the NS equations. Moreover, in conjunction with parallel flow assumptions, the linearized NS equations have enabled modal and non-modal stability analysis of spatially evolving flows via eigenvalue decomposition of the Orr-Sommerfeld equations [9]. However, such models do not accurately capture the effect of the spatially evolving base flow on the stability of the boundary layer. Global stability analysis addresses this issue by accounting for the spatially varying nature of the base flow in addition to spatial discretization in the inhomogeneous directions [10]–[12]. Although accurate, this approach is prohibitively expensive for flow control and optimization.

At sufficiently large amplitudes primary disturbances that are instigated via receptivity processes involving external or internal perturbations [13] lead to the parametric excitation of secondary instability mechanisms. Such mechanisms in turn trigger a strong energy transfer from the mean flow into secondary modes [14]. The physics of such transition mechanisms has been previously studied using Floquet analysis [14]–[16] and the Parabolized Stability Equations (PSE) [17]–[19].

The PSE were introduced to account for non-parallel and nonlinear effects which was not possible using eigenvalue problems arising from the Orr-Sommerfeld equations. In particular, the PSE were developed as a means to refine predictions of parallel flow analysis in slowly varying flows [19], [20], e.g., the laminar boundary layer flow. In general, the linear PSE and their stochastically forced variant provide reasonable predictions for the evolution of primary modes such as Tollmien-Schlichting (TS) waves in boundary layer flow [18], [21]. However, secondary growth mechanisms that lead to laminar-turbulent transition of the boundary layer flow originate from mode interactions [18].

In the transitional boundary layer, primary instability mechanisms cause perturbations to grow to finite amplitudes and saturate at steady or quasi-steady states. Floquet stability analysis identifies secondary instability modes as the eigenmodes of the linearized NS equations around a modified base flow profile that contains the spatially periodic primary velocity fluctuations. In the corresponding eigenvalue problem, the operators inherit a lifted representation from the spatial periodicity of the base flow [22] and as a result capture primary-secondary mode interactions. Such lifted representations also appear in the modeling of periodic flow control strategies in wall-bounded shear flows [7], [23], [24].

In this paper, we propose a framework which utilizes Floquet theory [25] to capture the dominant mode interactions and adopts the assumptions of the linear PSE to account for the spatial evolution of the base flow. The resulting equations

Financial support from the National Science Foundation under Award CMMI 1739243 and the Air Force Office of Scientific Research under Award FA9550-16-1-0009 is gratefully acknowledged.

Wei Ran is with the Department of Aerospace and Mechanical Engineering, University of Southern California, Los Angeles, CA 90089. Armin Zare and Mihailo R. Jovanović are with the Ming Hsieh Department of Electrical Engineering, University of Southern California, Los Angeles, CA 90089. M. J. Philipp Hack is with the Center for Turbulence Research, Stanford University, Stanford, CA 94305. E-mails: wran@usc.edu, armin.zare@usc.edu, philipp.hack@stanford.edu, mihailo@usc.edu.

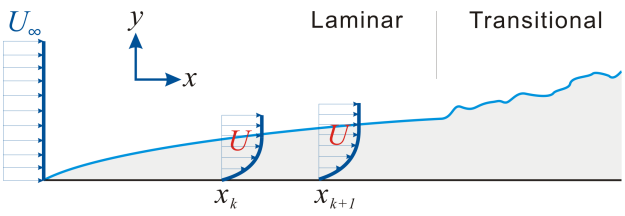

Fig. 1. Geometry of a transitional boundary layer flow.

are advanced downstream via a marching procedure. Our framework thus inherits the ability to account for mode interactions from Floquet theory while maintaining the low-complexity of the linear PSE. As a result, our models not only replicate the dominant physics of typical transitional flows, they are convenient for flow control design.

Our presentation is organized as follows. In Section II, we describe the linearized NS equations and the linear PSE. In Section III, we derive the proposed parabolized Floquet equations and explain our modeling framework. In Section IV, we use our framework to study the formation of streaks in the boundary layer flow. We conclude with remarks and future directions in Section V.

II. Background

In this section, we present the equations that govern the dynamics of flow fluctuations in incompressible flows of Newtonian fluids and provide details on our proposed model for the downstream marching of spatially growing fluctuations in boundary layer flows.

In a flat-plate boundary layer, with geometry shown in Fig. 1, the dynamics of flow fluctuations around a two-dimensional base flow profile $\bar{\mathbf{u}} = [U(x,y) \;\; V(x,y) \;\; 0]^T$ are governed by the linearized NS equations

$$\begin{aligned} \mathbf{v}_t &= -(\nabla\cdot\bar{\mathbf{u}})\,\mathbf{v} - (\nabla\cdot\mathbf{v})\,\bar{\mathbf{u}} - \nabla p + \frac{1}{Re_0}\Delta\mathbf{v} \\ 0 &= \nabla\cdot\mathbf{v}, \end{aligned} \tag{1}$$

where $\mathbf{v} = [u \;\; v \;\; w]^T$ is the vector of velocity fluctuations, p denotes pressure fluctuations, and u, v, and w represent streamwise (x), wall-normal (y), and spanwise (z) components of the fluctuating velocity field, respectively. The Reynolds number is defined as $Re_0 = U_\infty\delta_0/\nu$, where $\delta_0 = \sqrt{\nu x_0/U_\infty}$ is the Blasius length scale at the inflow x_0, U_∞ is the free-stream velocity, and ν is the kinematic viscosity. Spatial coordinates are non-dimensionalized by δ_0, velocities by U_∞, time by δ_0/U_∞, and pressure by ρU_∞^2, where ρ is the fluid density.

It is customary to use the parallel-flow approximation to study the stability of boundary layer flows to small amplitude perturbations [9]. Moreover, by leveraging the additional degree of freedom introduced by Floquet theory [25], such models have been used to investigate secondary instabilities that inflict transition [9], [14]. However, this approximation does not accurately capture the effect of the spatially-evolving base flow on the stability of the boundary layer. This issue can be addressed using global stability analysis which accounts for the spatially varying nature of the base flow in addition to the spatial discretization of all inhomogeneous directions. Nevertheless, global analysis of spatially-evolving flows is prohibitively expensive for analysis and control purposes.

To provide a convenient framework for the spatial marching of velocity fluctuations in weakly nonlinear scenarios, the parabolized stability equations (PSE) were introduced to refine predictions of parallel flow analysis [18]–[20]. These equations are obtained by removing the dominant elliptic components from the NS equations and are significantly more efficient than conventional flow simulations based on the governing equations.

In weakly non-parallel flows, e.g., the pre-transitional boundary layer, flow fluctuations can be separated into slowly and rapidly varying components [20]. This is achieved by considering the following decomposition for the fluctuation field $\mathbf{q} = [u \;\; v \;\; w \;\; p]^T$ in (1). For a specific spanwise wavenumber and temporal frequency pair (β,ω), we consider

$$\begin{aligned} \mathbf{q}(x,y,z,t) &= \hat{\mathbf{q}}(x,y)\,\chi(x,z,t) + \text{complex conjugate}, \\ \chi(x,z,t) &= \exp\left(\mathrm{i}\left(\alpha(x)\,x + \beta\,z - \omega\,t\right)\right), \\ \theta(x) &= \int_{x_0}^{x}\alpha(\xi)\,\mathrm{d}\xi, \end{aligned}$$

where $\hat{\mathbf{q}}(x,y)$ and $\chi(x,z,t)$ are the shape and phase functions and $\alpha(x)$ is the streamwise varying generalization of the wavenumber [20]. This decomposition separates slowly ($\hat{\mathbf{q}}(x,y)$) and rapidly ($\chi(x,z,t)$) varying scales in the streamwise direction. The ambiguity arising from the streamwise variation of both $\hat{\mathbf{q}}$ and α is resolved by imposing the condition $\int_{\Omega_y}\hat{\mathbf{q}}^*\hat{\mathbf{q}}_x\,\mathrm{d}y = 0$ [20]. This condition has also been used to develop iterative schemes for updating α at each streamwise location x; see [18, Section 3.2.5]. Based on this, the linearized NS equations are parabolized with the assumption that the streamwise variation of $\hat{\mathbf{q}}$ and α are sufficiently small to neglect $\hat{\mathbf{q}}_{xx}$, α_{xx}, $\alpha_x\hat{\mathbf{q}}_x$, α_x/Re_0. This amounts to the removal of terms of $O(1/Re_0^2)$ and higher, and thus the dominant source of ellipticity from the NS equations. The linear PSE take the form

$$\mathbf{L}\,\hat{\mathbf{q}} + \mathbf{M}\,\hat{\mathbf{q}}_x = 0, \tag{2}$$

where expressions for the operator-valued matrices $\mathbf{L}$ and $\mathbf{M}$ can be found in [18].

We next propose a two-step modeling procedure which combines Floquet theory with linear PSE to study the role of mode interactions in weakly nonlinear mechanisms that arise in spatially evolving flows.

III. Parabolized Floquet equations

In the transitional boundary layer flow, primary instabilities can cause perturbations to grow to finite amplitudes and saturate at steady or quasi-steady states. Secondary stability

analysis examines the linear stability of fluctuations in the modulated flow state, and it thus considers linearization around the modified base flow

$$\bar{\mathbf{u}} \;=\; \mathbf{u}_0 \;+\; \mathbf{u}_{\mathrm{pr}}, \tag{3}$$

where $\mathbf{u}_0$ denotes the original base flow and $\mathbf{u}_{\mathrm{pr}}$ represents the primary fluctuation field. Due to the spatial periodicity of the primary fluctuations, the new stability problem involves equations with spatially periodic coefficients, for which solutions can be found using Floquet analysis. When the spatially periodic flow structures are superposed to the Blasius boundary layer profile, the modified base flow (3) takes the form

$$\bar{\mathbf{u}}(x,y,z,t) \;=\; \sum_{m=-\infty}^{\infty} \mathbf{u}_m(x,y)\,\phi_m(x,z,t), \tag{4}$$

where $\mathbf{u}_0 = [\,U_B(x,y)\;\; V_B(x,y)\;\; 0\,]^T$ represents the Blasius boundary layer profile, $\phi_0 = 1$, $\mathbf{u}_m$ and ϕ_m $(m \neq 0)$ denote the shape and phase functions of the harmonics that constitute the primary fluctuation field (e.g. streaks), and $\mathbf{u}_m^* = \mathbf{u}_{-m}$. Subsequently, the fluctuations around the modified base flow $\bar{\mathbf{u}}$ are given by the similarly formed ansatz

$$\mathbf{q}(x,y,z,t) \;=\; \sum_{n=-\infty}^{\infty} \hat{\mathbf{q}}_n(x,y)\,\chi_n(x,z,t), \tag{5}$$

where $\hat{\mathbf{q}}_n(x,y)$ and $\chi_n(x,z,t)$ denote the shape and phase functions of the corresponding harmonics that constitute the fluctuation field $\mathbf{q}$. In Eq. (5), the phase functions χ_n share a uniform spatial growth rate, i.e., all modes share a uniform streamwise wavenumber $\alpha(x)$.

Following the PSE assumption, the parabolized linear NS equations that govern the dynamics of fluctuations around the modified base flow (3) give rise to the Parabolized Floquet Equations (PFE)

$$\mathbf{L}_F\,\hat{\mathbf{q}} \;+\; \mathbf{M}_F\,\hat{\mathbf{q}}_x \;=\; 0. \tag{6}$$

Here, the state

$$\hat{\mathbf{q}} \;=\; [\;\cdots\;\; \hat{\mathbf{q}}_{n-1}^T\;\; \hat{\mathbf{q}}_n^T\;\; \hat{\mathbf{q}}_{n+1}^T\;\; \cdots\;]^T,$$

contains all harmonics in the spanwise direction z with

$$\hat{\mathbf{q}}_n \;=\; [\,\hat{u}_n\;\; \hat{v}_n\;\; \hat{w}_n\;\; \hat{p}_n\,]^T,$$

and $\mathbf{L}_F$ and $\mathbf{M}_F$ inherit the following lifted representation from the periodicity of the base flow [22]

$$\mathbf{L}_F := \begin{bmatrix} \ddots & \vdots & \vdots & \vdots & \iddots \\ \cdots & \mathbf{L}_{n-1,0} & \mathbf{L}_{n-1,+1} & \mathbf{L}_{n-1,+2} & \cdots \\ \cdots & \mathbf{L}_{n,-1} & \mathbf{L}_{n,0} & \mathbf{L}_{n,+1} & \cdots \\ \cdots & \mathbf{L}_{n+1,-2} & \mathbf{L}_{n+1,-1} & \mathbf{L}_{n+1,0} & \cdots \\ \iddots & \vdots & \vdots & \vdots & \ddots \end{bmatrix}.$$

The operator $\mathbf{L}_{i,j}$ captures the contribution of the jth harmonic $\hat{\mathbf{q}}_j$ on the dynamics of the ith harmonic $\hat{\mathbf{q}}_i$ induced by the periodicity of the base flow.

To model the effect of mode interactions in weakly nonlinear regimes we consider the following two-step procedure:

1) The linear PSE are used to march the fundamental harmonic and obtain its corresponding velocity profile $\mathbf{u}_{\mathrm{pr}}$ at each location in the streamwise direction.
2) The PFE are used to march all harmonics $\hat{\mathbf{q}}$ and obtain the evolution of velocity fluctuations around the modified base flow $\bar{\mathbf{u}}$.

The PFE are thus used to study the effect of dominant harmonic interactions on the growth of disturbances in the streamwise direction. The schematic diagram in Fig. 2 illustrates our modeling procedure.

Comparison with nonlinear PSE

In contrast to the nonlinear PSE, which treat the interaction of various modes as a nonlinear input forcing, the PFE introduced in Eq. (6) account for a subset of *essential* interactions between the primary and secondary modes while maintaining the linear progression of the governing equations. Moreover, from a conceptual standpoint, it is much easier to implement the PFE than the nonlinear PSE. This is because the PFE do not involve the inner iterations that are required to update the nonlinear forcing term. Moreover, the uniform growth rate considered by PFE allows for the update of a uniform streamwise wavenumber $\alpha(x)$ for all harmonics. While this feature may introduce inaccuracies to the evolution of disturbances, in Section IV we show that the PFE can indeed provide correct predictions of the evolution of laminar streaks in boundary layer flow.

In addition, in many scenarios, e.g., the H-type transition scenario in boundary layer flow, the growth of nonlinear terms can cause the convergence of the nonlinear PSE to deteriorate. Specifically, after secondary modes grow to the same order of magnitude as primary modes, the nonlinear terms become dominant and at some point update schemes for $\alpha(x)$ fail to converge. While the location at which update schemes fail to converge has been previously used to predict the onset of transition [26], there have been some efforts to suppress the feedback from secondary modes to primary modes and maintain the march of nonlinear PSE through the transitional region [18, Section 3.4.3]. The framework proposed in this paper allows for the formal investigation of such effects; see [27] for the application of the PFE in predicting the growth of subharmonic modes of the H-type transition scenario.

IV. Streamwise elongated streaks

The bypass transition process refers to transition emanating from non-modal growth mechanisms and includes the algebraic or transient growth of streamwise elongated modes (streaks) [9]. In fact, streamwise elongated streaks are among the most important physical structures that appear as a result of bypass transition in boundary layer flows.

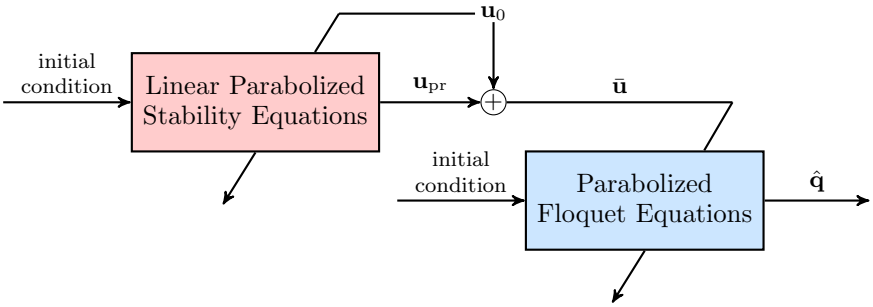

Fig. 2. The PFE are triggered with a primary disturbance $\mathbf{u}_{\rm pr}$ that results from linear PSE and modulates the base flow. The diagonal lines represent base flow terms that enter as coefficients into the linear PSE and PFE.

Secondary instability analysis of saturated streaks has been previously used to analyze the breakdown stage in the transition process [15], [16], [28]. In this section, we utilize Floquet theory in an earlier stage of the transition process and before the breakdown of streaks. We consider the case in which interactions between various spanwise harmonics contribute to a significant mean-flow distortion (MFD) that in turn affects the energy balance among various harmonics that form streaks. While the linear PSE fail to predict such a phenomenon, we demonstrate how the PFE provide the means to predict the correct trend in the MFD as well as the resulting velocity distribution.

A. Setup

Starting from an initial condition identified as the optimal disturbance in triggering algebraic growth in the Blasius boundary layer flow [29], we extract the spatial growth predicted by the evolution of the primary harmonic via linear PSE. We use the solution to this primary linear PSE computation to augment the Blasius boundary layer profile $\mathbf{u}_0$ in the base flow for the subsequent PFE computation

$$\begin{aligned} U(x,y) &= U_B(x,y) + U_S(x,y)\,\mathrm{e}^{\mathrm{i}\beta z} + U_S^*(x,y)\,\mathrm{e}^{-\mathrm{i}\beta z} \\ V(x,y) &= V_B(x,y) \\ W(x,y) &= 0. \end{aligned} \tag{7}$$

Since the velocity field of streamwise elongated streaks is dominated by its streamwise component, we only use the streamwise component of the solution to linear PSE, $U_S(x,y)$, in (7). The state in the PFE takes the form of the following Fourier expansion

$$\mathbf{q}(x,y,z,t) = \mathrm{e}^{\mathrm{i}(\alpha(x)x-\omega t)} \sum_{n=-\infty}^{\infty} \hat{\mathbf{q}}_n(x,y)\,\mathrm{e}^{\mathrm{i}n\beta z}, \tag{8}$$

where $\hat{\mathbf{q}}_0$ is the MFD and higher-order harmonics in the spanwise direction represent various streaks of wavelength $2\pi/(n\beta)$. Operators $\mathbf{L}_F$ and $\mathbf{M}_F$ in Eq. (6) are provided in the appendix.

B. Nonlinear evolution of streaks

The physics of the streamwise growing streaky structure is comprised of various harmonics in the spanwise direction. The mean flow distortion $\hat{\mathbf{q}}_0$ is generated as a result of the nonlinearity of the NS equations which cause interactions between various harmonics. To investigate the result of such interactions, we consider various truncations of the bi-infinite state $\hat{\mathbf{q}}$ to $2N+1$ harmonics in z, i.e., $n=-N,\cdots,N$. In this study, a truncation with $N=3$ proved sufficient to capture the relevant physics. We consider a rectangular computational domain with $L_x \times L_y = 2000 \times 60$, where L_x and L_y denote the length of the computational domain in the streamwise and wall-normal directions, respectively. Homogenous Dirichlet boundary conditions are enforced in the wall-normal direction, and differential operators are discretized using a pseudospectral scheme with $N_y = 80$ Chebyshev collocation points in the wall-normal direction [30]. To march the linear PSE and PFE downstream, we adopt an implicit Euler scheme with step-size $\Delta x = 15$. Our computational experiments show that similar predictions can be achieved with appreciably coarser computational grids, e.g., $N_y = 40$ and $\Delta x = 30$.

The temporal frequency, streamwise wavenumber, and fundamental spanwise wavenumber are set to $\omega = 0$, $\alpha = -10^{-6}\mathrm{i}$, and $\beta = 0.4065$, respectively. Note that $\mathrm{Re}\{\alpha\} = 0$ corresponds to infinitely long structures in the streamwise direction. We initialize the PFE computation at $Re_0 = 467$ (this corresponds to the streamwise location $x_0 = 467$) and zero initial conditions for all $\hat{\mathbf{q}}_n$ with $n \neq \pm 1$. The fundamental harmonic $\hat{\mathbf{q}}_{\pm 1}$ is initialized with the same initial condition as the primary linear PSE computations. Since this case study considers the evolution of perturbations with a slowly varying streamwise wavenumber α we assume $\alpha_x = 0$ for both the primary linear PSE and the subsequent PFE computations [31].

To verify the predictions of our framework, we also performed numerical simulations of the nonlinear NS equations with the same initial conditions. The numerical simulations were conducted using a second-order finite volume code with $1024 \times 192 \times 192$ grid points in the streamwise, wall-normal, and spanwise dimensions, respectively.

Figure 3 compares the result of Direct Numerical Simulation (DNS) of the NS equations and the predictions of PFE and linear PSE. As shown in this figure, the evolution of all harmonics involves an initial algebraic growth followed

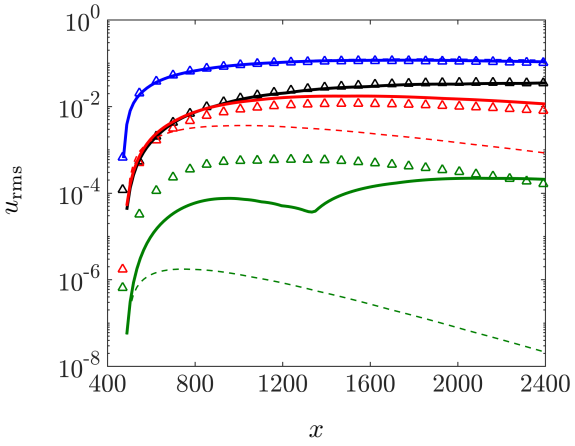

Fig. 3. The rms amplitudes of the streamwise velocity components for various harmonics with $\omega = 0$ and $\beta = 0.4065$ resulting from DNS ($\triangle$), PFE ($-$), and linear PSE ($--$). The MFD, first, second, and third harmonics are shown in black, blue, red, and green, respectively.

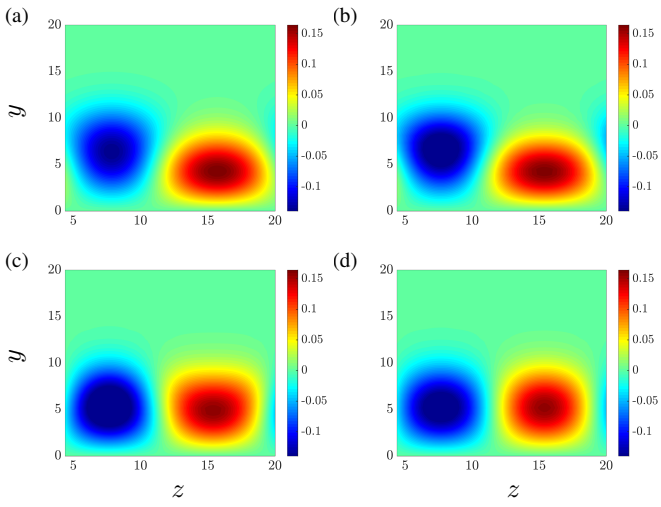

Fig. 4. Cross-plane contours of the streamwise velocity of the streak comprised of all harmonics in the spanwise direction at $x = 2400$ resulting from DNS (a), PFE with (b) and without (c) the MFD, and Linear PSE (d).

by saturation. The solution to the linear PSE accurately predicts the evolution of the fundamental spanwise harmonic; cf. Eq. (8). Subsequently, the PFE accurately predict the growth of the dominant harmonics, and especially the MFD. While a discrepancy is observed for the third harmonic, its contribution to the overall structure of the streak is negligible. Since all harmonics other than $\hat{\mathbf{q}}_{\pm 1}$ were initialized with zero, it is worth noting that the reasonable prediction of growth rates and generation of the MFD component would not have been possible without accounting for the interaction between various harmonics.

Figure 4 shows the cross-plane spatial structure of the streak comprised of all harmonics in the spanwise direction at $x = 2400$. Figure 4(b) demonstrates perfect matching with the result of DNS. As shown in Fig. 4(c), the velocity distribution would not be correct in the absence of the MFD. Moreover, as it is clear from comparing Figs. 4(a) and 4(d), there is a significant discrepancy between the shape of the structures in the cross-plane if the interaction between modes is not taken into account. Due to the significant relative amplitude of the first (fundamental) harmonic compared with the second and third harmonics, the velocity distribution resulting from the linear PSE are dominated by the structure of the first harmonic. In addition, in the absence of interactions between harmonics, the linear PSE would not be able to generate the MFD and would result in inaccurate predictions for the amplitude of higher-order harmonics; see dashed lines in Fig. 3.

V. Concluding Remarks

We have combined Floquet theory and the linear PSE to develop the PFE which can be used to conveniently march primary and secondary instability modes while accounting for dominant mode interactions. This framework involves two steps: (i) the primary modes are marched using the linear PSE; (ii) weakly nonlinear effects and interaction of modes are captured via the PFE. Nonlinear effects are captured by dominant interactions among various harmonics of the fluctuation field which includes the primary harmonics from step (i). The PFE involve a convenient linear march of various harmonics and is of low-complexity. It is thus better suited for the purpose of analysis and control synthesis than conventional nonlinear models. We use the proposed framework for the secondary instability analysis of streamwise elongated streaks in the laminar boundary layer flow. Our results demonstrate good agreement with numerical simulations of the nonlinear equations. We refer the interested reader to [27] for a more detailed description of the PFE framework and an in-depth discussion on the utility of this model in predicting subharmonic growth in H-type transition.

We note that the overall performance of the proposed method relies on a reasonable prediction of the evolution of the primary modes using linear PSE. When the linear PSE cannot accurately predict the evolution of the primary modes, an additional source of white or colored stochastic excitation can be used to replicate the effect of nonlinearities and improve predictions of the linear PSE; see [21, Section IV]. For this purpose, the spatio-temporal spectrum of stochastic excitation sources can be identified using the recently developed theoretical framework outlined in [8], [32]. Such an extension of the current PFE model is a topic for future research.

Appendix

The operators $\mathbf{L}_{n,m}$ and $\mathbf{M}_{n,m}$ in $\mathbf{L}_F$ and $\mathbf{M}_F$ from Eq. (6) are of the form:

$$\mathbf{L}_{n,0} = \begin{bmatrix} \Gamma_n - \partial_y V_B & \partial_y U_B & 0 & \mathrm{i}\alpha \\ 0 & \Gamma_n + \partial_y V_B & 0 & \partial_y \\ 0 & 0 & \Gamma_n & \mathrm{i}n\beta \\ \mathrm{i}\alpha & \partial_y & \mathrm{i}n\beta & 0 \end{bmatrix},$$

$$\mathbf{L}_{n,-1} = \begin{bmatrix} \mathrm{i}\alpha\, U_S & \partial_y U_S & \mathrm{i}\beta\, U_S & 0 \\ 0 & \mathrm{i}\alpha\, U_S & 0 & 0 \\ 0 & 0 & \mathrm{i}\alpha\, U_S & 0 \\ 0 & 0 & 0 & 0 \end{bmatrix},$$

$$\mathbf{L}_{n,+1} = \begin{bmatrix} \mathrm{i}\alpha\, U_S^* & \partial_y U_S^* & -\mathrm{i}\beta\, U_S^* & 0 \\ 0 & \mathrm{i}\alpha\, U_S^* & 0 & 0 \\ 0 & 0 & \mathrm{i}\alpha\, U_S^* & 0 \\ 0 & 0 & 0 & 0 \end{bmatrix},$$

and

$$\mathbf{M}_{n,0} = \begin{bmatrix} U_B - \dfrac{2\mathrm{i}\alpha}{Re} & 0 & 0 & 0 \\ 0 & U_B - \dfrac{2\mathrm{i}\alpha}{Re} & 0 & 0 \\ 0 & 0 & U_B - \dfrac{2\mathrm{i}\alpha}{Re} & 0 \\ 0 & 0 & 0 & 0 \end{bmatrix},$$

$$\mathbf{M}_{n,-1} = \begin{bmatrix} U_S & 0 & 0 & 0 \\ 0 & U_S & 0 & 0 \\ 0 & 0 & U_S & 0 \\ 0 & 0 & 0 & 0 \end{bmatrix},$$

$$\mathbf{M}_{n,+1} = \begin{bmatrix} U_S^* & 0 & 0 & 0 \\ 0 & U_S^* & 0 & 0 \\ 0 & 0 & U_S^* & 0 \\ 0 & 0 & 0 & 0 \end{bmatrix},$$

where

$$\Gamma_n = -\frac{1}{Re}[\partial_{yy} - \alpha^2 + (n\beta)^2] + [-\mathrm{i}\omega + \mathrm{i}\alpha\, U_B + V_B \partial_y].$$

REFERENCES

[1] B. R. Noack, M. Morzyński, and G. Tadmor, *Reduced-order modelling for flow control*, ser. CISM Courses and Lectures. Springer, 2011, vol. 528.

[2] J. Kim and T. R. Bewley, "A linear systems approach to flow control," *Annu. Rev. Fluid Mech.*, vol. 39, pp. 383–417, 2007.

[3] B. F. Farrell and P. J. Ioannou, "Stochastic forcing of the linearized Navier-Stokes equations," *Phys. Fluids A*, vol. 5, no. 11, pp. 2600–2609, 1993.

[4] B. Bamieh and M. Dahleh, "Energy amplification in channel flows with stochastic excitation," *Phys. Fluids*, vol. 13, no. 11, pp. 3258–3269, 2001.

[5] M. R. Jovanović and B. Bamieh, "Componentwise energy amplification in channel flows," *J. Fluid Mech.*, vol. 534, pp. 145–183, July 2005.

[6] Y. Hwang and C. Cossu, "Linear non-normal energy amplification of harmonic and stochastic forcing in the turbulent channel flow," *J. Fluid Mech.*, vol. 664, pp. 51–73, 2010.

[7] R. Moarref and M. R. Jovanović, "Model-based design of transverse wall oscillations for turbulent drag reduction," *J. Fluid Mech.*, vol. 707, pp. 205–240, September 2012.

[8] A. Zare, M. R. Jovanović, and T. T. Georgiou, "Colour of turbulence," *J. Fluid Mech.*, vol. 812, pp. 636–680, February 2017.

[9] P. J. Schmid and D. S. Henningson, *Stability and Transition in Shear Flows*. New York: Springer-Verlag, 2001.

[10] U. Ehrenstein and F. Gallaire, "On two-dimensional temporal modes in spatially evolving open flows: the flat-plate boundary layer," *J. Fluid Mech.*, vol. 536, pp. 209–218, 2005.

[11] E. Åkervik, U. Ehrenstein, F. Gallaire, and D. Henningson, "Global two-dimensional stability measures of the flat plate boundary-layer flow," *Euro. J. Mech.-B/Fluids*, vol. 27, no. 5, pp. 501–513, 2008.

[12] P. Paredes, R. Gosse, V. Theofilis, and R. Kimmel, "Linear modal instabilities of hypersonic flow over an elliptic cone," *J. Fluid Mech.*, vol. 804, pp. 442–466, 2016.

[13] Y. S. Kachanov, "Physical mechanisms of laminar-boundary-layer transition," *Annu. Rev. Fluid Mech.*, vol. 26, no. 1, pp. 411–482, 1994.

[14] T. Herbert, "Secondary instability of boundary layers," *Ann. Rev. Fluid Mech.*, vol. 20, pp. 487–526, 1988.

[15] P. Andersson, L. Brandt, A. Bottaro, and D. S. Henningson, "On the breakdown of boundary layer streaks," *J. Fluid Mech.*, vol. 428, pp. 29–60, 2001.

[16] L. Brandt, "Numerical studies of bypass transition in the Blasius boundary layer," Ph.D. dissertation, Royal Institute of Technology, Stockholm, Sweden, 2003.

[17] R. Joslin, C. Streett, and C. Chang, "Spatial direct numerical simulation of boundary-layer transition mechanisms: Validation of PSE theory," *Theor. & Comput. Fluid Dyn.*, vol. 4, no. 6, pp. 271–288, 1993.

[18] T. Herbert, "Parabolized stability equations," in *Special Course on Progress in Transition Modelling*. AGARD Rep., 1994, ch. 4, pp. 1–34, No. 793.

[19] T. Herbert, "Parabolized stability equations," *Annu. Rev. Fluid Mech.*, vol. 29, no. 1, pp. 245–283, 1997.

[20] F. P. Bertolotti, T. Herbert, and P. R. Spalart, "Linear and nonlinear stability of the Blasius boundary layer," *J. Fluid Mech.*, vol. 242, pp. 441–474, 1992.

[21] W. Ran, A. Zare, M. J. P. Hack, and M. R. Jovanović, "Low-complexity stochastic modeling of spatially-evolving flows," in *Proceedings of the 2017 American Control Conference*, 2017, pp. 3815–3820.

[22] M. Fardad, M. R. Jovanović, and B. Bamieh, "Frequency analysis and norms of distributed spatially periodic systems," *IEEE Trans. Automat. Control*, vol. 53, no. 10, pp. 2266–2279, November 2008.

[23] M. R. Jovanović, "Turbulence suppression in channel flows by small amplitude transverse wall oscillations," *Phys. Fluids*, vol. 20, no. 1, p. 014101 (11 pages), January 2008.

[24] R. Moarref and M. R. Jovanović, "Controlling the onset of turbulence by streamwise traveling waves. Part 1: Receptivity analysis," *J. Fluid Mech.*, vol. 663, pp. 70–99, November 2010.

[25] S. Bittanti and P. Colaneri, *Periodic systems: filtering and control*. Springer Science & Business Media, 2009, vol. 5108985.

[26] M. J. P. Hack and P. Moin, "Towards modeling boundary layer transition in large-eddy simulations," in *Annual Research Briefs*, Center for Turbulence Research, Stanford University, 2015, pp. 137–144.

[27] W. Ran, A. Zare, M. J. P. Hack, and M. R. Jovanović, "Modeling mode interactions in boundary layer flows via Parabolized Floquet Equations," *Phys. Rev. Fluids*, 2017, submitted; also arXiv:1712.02024.

[28] M. J. P. Hack and T. A. Zaki, "Streak instabilities in boundary layers beneath free-stream turbulence," *J. Fluid Mech.*, vol. 741, pp. 280–315, 2014.

[29] M. J. P. Hack and P. Moin, "Algebraic disturbance growth by interaction of Orr and lift-up mechanisms," *J. Fluid Mech.*, vol. 829, pp. 112–126, 2017.

[30] J. A. C. Weideman and S. C. Reddy, "A MATLAB differentiation matrix suite," *ACM Trans. Math. Software*, vol. 26, no. 4, pp. 465–519, December 2000.

[31] A. Towne, "Advancements in jet turbulence and noise modeling: accurate one-way solutions and empirical evaluation of the nonlinear forcing of wavepackets," Ph.D. dissertation, California Institute of Technology, 2016.

[32] A. Zare, Y. Chen, M. R. Jovanović, and T. T. Georgiou, "Low-complexity modeling of partially available second-order statistics: theory and an efficient matrix completion algorithm," *IEEE Trans. Automat. Control*, vol. 62, no. 3, pp. 1368–1383, March 2017.